Modulation of atomic positions in $CaCu_xMn_{7-x}O_{12}$ ($x \leq 0.1$)

W. Sławiński,[a] R. Przeniosło,[a]* I. Sosnowska,[a]* M. Bieringer,[b] I. Margiolaki[c] and E. Suard[d]

[a]Institute of Experimental Physics, University of Warsaw, 00-681 Warsaw, Hoża 69, Poland, [b]Department of Chemistry, University of Manitoba, Winnipeg, Canada R3T 2N2, [c]European Synchrotron Radiation Facility, BP220, Grenoble CEDEX, F-38043, France, and [d]Institut Laue–Langevin, 6 rue Jules Horowitz, BP-156X 38 042 Grenoble, France

Correspondence e-mail: radek@fuw.edu.pl, izabela@fuw.edu.pl

The modulation of atomic positions in $CaCu_xMn_{7-x}O_{12}$ ($x = 0$ and 0.1) was studied using synchrotron radiation powder diffraction below 250 and 220 K, respectively. The copper-rich member $CaCu_xMn_{7-x}O_{12}$ ($x = 0.23$) does not show any modulation of the atomic positions at temperatures as low as 10 K. Using low-temperature neutron powder diffraction the modulation of the magnetic moments of Mn ions in $CaCu_xMn_{7-x}O_{12}$ ($x = 0$, 0.1 and 0.23) has been investigated. Long-range modulated magnetic ordering in $CaCu_xMn_{7-x}O_{12}$ ($x = 0$, 0.1 and 0.23) is observed below 90.4, 89.2 and 78.1 K. $(0,0,q_p)$ and $(0,0,q_m)$ are the propagation vectors describing the modulations of the atomic positions and the magnetic moments. For $CaCu_xMn_{7-x}O_{12}$ ($x = 0$ and 0.1) the magnetic modulation and atomic modulation lengths are related by a factor of 2 satisfying the relation $(1 - q_p) = 2(1 - q_m)$.

1. Introduction

The manganates of composition $CaCu_xMn_{7-x}O_{12}$ are derived from the parent compound $CaMn_7O_{12}$ and display complex structural and magnetic properties. $CaMn_7O_{12}$ undergoes a charge and/or atomic positions modulation below 250 K, as shown by synchrotron radiation diffraction experiments (Sławiński *et al.*, 2008). Upon further cooling $CaMn_7O_{12}$ undergoes modulated magnetic ordering at $T_N = 90$ K, followed by a magnetic phase transition at $T_C = 50$ K associated with changes of the magnetic modulation vector and the magnetic-ordering coherence length (Przeniosło *et al.*, 1999). The changes of these modulated orderings are associated with several anomalies of the macroscopic properties of $CaMn_7O_{12}$. Between 250 and 150 K the dielectric constant of $CaMn_7O_{12}$ decreases by four orders of magnitude (Yáñez-Vilar *et al.*, 2005; Castro-Couceiro *et al.*, 2006). The transition at $T_N = 90$ K causes anomalies in the specific heat, magnetization and thermal expansion (Volkova *et al.*, 2005) and has also been observed with muon spin rotation (Prodi *et al.*, 2006) and Mössbauer spectroscopy (Presniakov *et al.*, 2007). The magnetic transition at $T_C = 50$ K in $CaMn_7O_{12}$ has been characterized by anomalies in the thermal expansion and specific heat (Volkova *et al.*, 2005). A recent study has identified magnetoelectric coupling in $CaMn_7O_{12}$ which is significantly enhanced below 50 K (Sánchez-Andújar *et al.*, 2009).

Doping the manganese sublattice in $CaMn_7O_{12}$ with copper increases the complexity of the system and even small doping levels have a profound impact on the physical properties of these $CaCu_xMn_{7-x}O_{12}$ compounds. Copper doping results in colossal magnetoresistance (Zeng *et al.*, 1999; Volkova *et al.*, 2006), which increases with Cu content in $CaCu_xMn_{7-x}O_{12}$. A review of the physical properties of $CaCu_xMn_{7-x}O_{12}$ is given in Vasiliev & Volkova (2007).

research papers

The present paper describes low-temperature, high-resolution powder diffraction studies of the $CaCu_xMn_{7-x}O_{12}$ family with relatively small Cu content: $x \leq 0.23$. The objective of these studies is to determine the atomic position modulations and magnetic moment modulations with particular emphasis on possible coupling between the magnetic and lattice degrees of freedom. The motivation for these studies comes from the complex physical properties of the parent compound $CaMn_7O_{12}$ and the copper-doped samples.

Figure 1
Results of the Rietveld refinement of the synchrotron radiation powder diffraction pattern of $CaMn_7O_{12}$ at 10 K. The solid points represent measured data, while the solid line represents the calculated diffraction pattern. The 2θ step was 0.002°. Below the graph there is a difference curve. The ticks indicate the positions for the Bragg peaks due to the crystal structure of $CaMn_7O_{12}$ (black – fundamental, green – satellite reflections) (top) and two impurity phases: $CaMn_4O_8$ (middle) and Mn_2O_3 (bottom). This figure is in colour in the electronic version of this paper.

2. Materials and methods

Bulk samples (approximately 5 g) of polycrystalline $CaCu_xMn_{7-x}O_{12}$ (x = 0.0, 0.10, 0.23) were prepared from stoichiometric amounts of $CaCO_3$ (CERAC, 99.995%), CuO (CERAC, 99.999%) and Mn_2O_3 (CERAC, 99.99%), as described in detail elsewhere (Sławiński et al., 2006).

Synchrotron radiation powder diffraction measurements were performed on the high-resolution powder diffraction beamline ID31 at the ESRF in Grenoble (Fitch, 2004). A monochromatic parallel beam is scattered from a powder sample sealed in a capillary. A bank of nine scintillation detectors is scanned vertically to measure the diffracted intensity as a function of 2θ. The detectors are $\sim 2°$ apart and each is preceded by an analyser crystal. The crystallographic information and the conditions for the synchrotron radiation diffraction experiments are given in the supplementary material.[1] The sample was measured in a spinning 0.5 mm glass capillary. Diffraction experiments were performed for several temperatures from 10 K up to 290 K by using a liquid helium-cooled cryostat. Using a synchrotron radiation wavelength of 0.39996 Å the angular range $2.0 \leq 2\theta \leq 47.9°$ was measured. The length of the scattering vector s analysed in the experiment was $0.13 \leq s \leq 2.03$ Å^{-1}, where $s = (2 \sin \theta)/\lambda$. The 2θ step was 0.002°. Owing to limited statistical accuracy the synchrotron radiation diffraction data were analysed only up to $2\theta = 41°$. A summary of crystal and experimental data are given in Table 1.

Neutron powder diffraction measurements of polycrystalline $CaCu_xMn_{7-x}O_{12}$ were performed on the diffractometer D20 at the ILL in Grenoble using a neutron wavelength of 2.418 Å. D20 is a medium-to-high-resolution two-axis diffractometer capable of producing a neutron flux of 10^8 s^{-1} cm^{-2} at the sample position. The monochromatic neutron beam is scattered on a powder sample sealed in a vanadium container. The 1536 detection cells of its curved linear position-sensitive detector (PSD) cover a continuous 2θ range of 153.6°. The powder sample was sealed in an 8 mm diameter cylindrical vanadium container and placed in a standard orange cryostat. Diffraction patterns were measured from 10 K up to 100 K with a heating rate of 0.37 K min^{-1}. Consecutive neutron powder diffraction patterns were measured for 3 min, which corresponds to a 1.1 K temperature interval. The length of the scattering vector s covered the range $0.064 \leq s \leq 0.716$ Å^{-1}.

3. Results

3.1. Atomic position modulation

Initial synchrotron radiation and neutron powder diffractograms of $CaCu_xMn_{7-x}O_{12}$ (x = 0, 0.1 and 0.23) were analysed with the Rietveld method (Rietveld, 1969) implemented in the program *FullProf* (Rodríguez-Carvajal, 1993).

---

[1] Supplementary data for this paper are available from the IUCr electronic archives (Reference: SN5079). Services for accessing these data are described at the back of the journal.
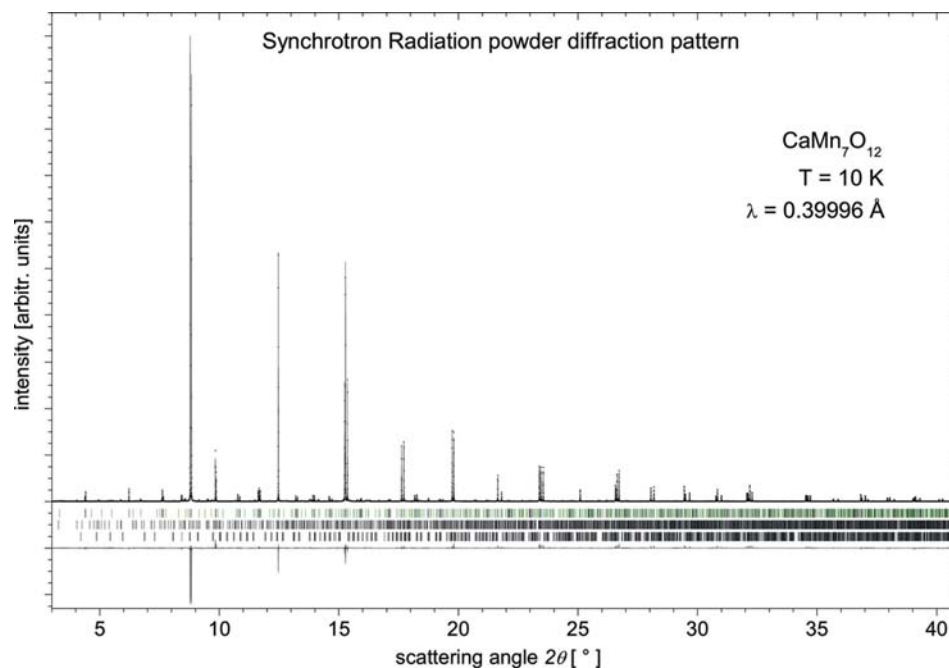
Table 1
Summary of crystal and experimental data.

Chemical formula	$CaMn_7O_{12}$	$CaCu_{0.1}Mn_{6.9}O_{12}$
Space group (average structure)	$R\bar{3}$ (No. 148)	$R\bar{3}$ (No. 148)
Superspace group	$R\bar{3}(00\gamma)0$ (No. 148.1)	$R\bar{3}(00\gamma)0$ (No. 148.1)
Temperature (K)	10.0	10.0
$a = b$ (Å)	10.44304 (1)	10.43374 (2)
c (Å)	6.343439 (5)	6.341994 (14)
V (Å^3)	599.1137 (7)	597.9105 (21)
Z	3	3
No. of main reflections ($|m| = 0$)	348	349
No. of main reflections ($|m| = 1$)	670	670
$(\sin\theta/\lambda)_{max}$	0.876	0.876
Calculated density (g cm^{-3})	5.1257	5.1441
$F(000)$	873	874
Linear absorption coefficient (mm^{-1})	2.155	2.186
λ (Å)	0.39996	0.39996
Diffractometer	ESRF ID-31	ESRF ID-31
Method of measurement	Debye–Scherrer	Debye–Scherrer
Modulation vector	$\mathbf{q}_p = 0.9203\,(1)\mathbf{c}^*$	$\mathbf{q}_p = 0.9052\,(2)\mathbf{c}^*$
Absorption correction	Cylindrical sample	Cylindrical sample
Refinement method	*JANA*2006	*JANA*2006

Table 2
Structural parameters of $CaMn_7O_{12}$ at $T = 10$ K.

The basic structure position and modulation parameters in relative coordinates [see equation (1)] and the isotropic ADP B (Å^2) are given. Results obtained by using the program *JANA*2006 (Petricek *et al.*, 2006).

| Atom	Position		B (Å^2)	A_i	B_i
Ca	x_0	0	0.46 (2)	–	–
	y_0	0		–	–
	z_0	0		−0.00905 (87)	–
Mn1	x_0	0.5	0.29 (1)	0.01062 (17)	–
	y_0	0		−0.00395 (24)	–
	z_0	0		0.00854 (28)	–
Mn2	x_0	0.5	0.29 (1)	0.00634 (14)	–
	y_0	0.5		0.00431 (18)	–
	z_0	0.5		−0.00255 (33)	–
Mn3	x_0	0	0.29 (1)	–	–
	y_0	0		–	–
	z_0	0.5		0.00686 (62)	–
O1	x_0	0.2231 (3)	0.41 (1)	0.00640 (49)	0.00334 (51)
	y_0	0.2742 (3)		0.00794 (48)	−0.00403 (48)
	z_0	0.0817 (3)		0.00037 (82)	−0.00042 (90)
O2	x_0	0.3416 (2)	0.41 (1)	0.00722 (47)	−0.00047 (67)
	y_0	0.5217 (2)		0.00077 (48)	−0.00011 (59)
	z_0	0.3414 (3)		0.00764 (82)	−0.00958 (80)

The basic crystal structure (non-modulated) of $CaMn_7O_{12}$ is described within the hexagonal setting of the space group $R\bar{3}$ as was first reported in Bochu *et al.* (1980). $CaMn_7O_{12}$ is a perovskite-like distorted structure $[CaMn_3][Mn_4][O_{12}]$ corresponding to ABO_3. The atomic positions obtained from the Rietveld refinement against synchrotron radiation powder diffraction patterns of $CaMn_7O_{12}$ at 10 K are given in Table 2. Isotropic Debye–Waller factors were refined independently for Ca, Mn and O. Two impurity phases were found in $CaMn_7O_{12}$: $CaMn_4O_8$ [2.65 (20)%] and Mn_2O_3 [2.32 (5)%].

Fig. 1 presents the Rietveld refinement of the synchrotron radiation powder diffraction pattern of $CaMn_7O_{12}$ at 10 K.

In our previous paper (Sławiński *et al.*, 2008) we described weak satellite peaks in the synchrotron radiation diffraction patterns of $CaCu_xMn_{7-x}O_{12}$ at temperatures below 250 K and proposed a possible indexing of those satellites. Representative parts of the synchrotron radiation diffraction patterns of $CaCu_xMn_{7-x}O_{12}$ ($x = 0$ and 0.1) with clearly identifiable satellite peaks are shown in Fig. 2. The satellite peaks are broader than the commensurate Bragg peaks observed for both samples.

The description of the modulation is given with the space group $R\bar{3}(00\gamma)0$ with the propagation vector $(0,0,q_p)$, where $q_p = 0.9213$ (1) for $CaMn_7O_{12}$. With this modulation wave-vector the reflection condition is (h, k, l, m): $-h + k + l = 3n$, where n is an integer. Either both or neither of the two satellites $(h, k, l + q_p)$ and $(h, k, l - q_p)$ are observed. Please note that the present indexing is different from that used in our previous paper with a propagation vector $(0, 0, 0.079\,(15))$ and reflections that fulfill the condition $-h + k + l + m = 3n$ (Sławiński *et al.*, 2008). A careful inspection of the diffraction data allowed us to determine a larger number of satellites compared with our previous study (Sławiński *et al.*, 2008). The synchrotron radiation diffraction pattern of $CaMn_7O_{12}$ shows 81 satellites (compared with 32 reported in Sławiński *et al.*, 2008), while for $CaCu_xMn_{7-x}O_{12}$ ($x = 0.1$) there are 20 satellites (compared with 13 reported in Sławiński *et al.*, 2008). There were no satellite peaks observed in the synchrotron radiation diffraction patterns of $CaCu_xMn_{7-x}O_{12}$ ($x = 0.23$).

The observed satellite intensities can be quantitatively described by assuming positional modulation of the ions in the
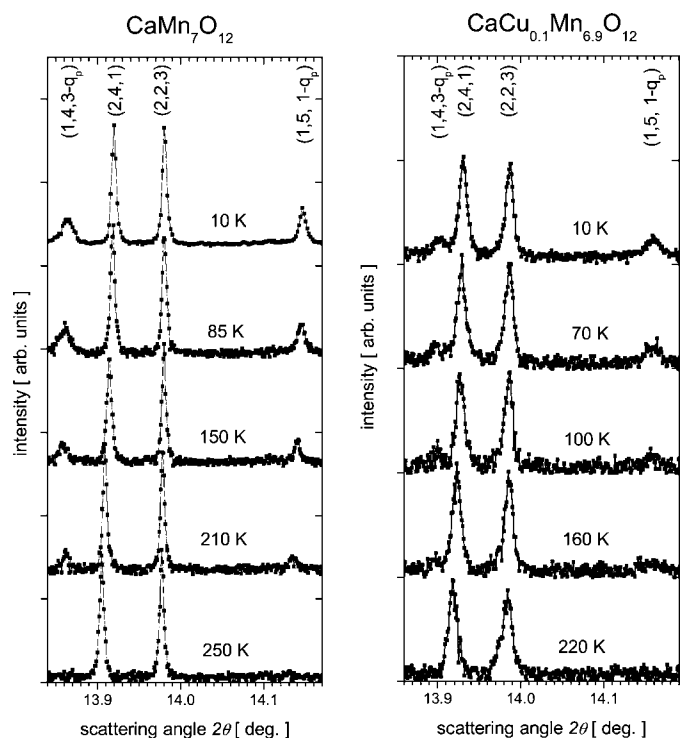
Figure 2
Representative parts of synchrotron radiation diffraction patterns of $CaMn_7O_{12}$ (left panel) and $CaCu_xMn_{7-x}O_{12}$, $x = 0.1$ (right panel), observed from 10 K up to room temperature in several temperature steps.

lattice. The parameters of the positional modulation have been found using the program *JANA*2006 (Petricek *et al.*, 2006). The charge modulation suggested in our earlier paper (Sławiński *et al.*, 2008) did not give satisfactory fits. The charge-modulation model (Sławiński *et al.*, 2008) is therefore not valid. The best agreement is obtained for a modulation of all the atomic positions in CaCu$_x$Mn$_{7-x}$O$_{12}$ given using the notation from van Smaalen (2007)

$$
\begin{aligned}
x(\bar{x}_4) &= x_0 + A_x \sin(2\pi\bar{x}_4) + B_x \cos(2\pi\bar{x}_4) + l_x \\
y(\bar{x}_4) &= y_0 + A_y \sin(2\pi\bar{x}_4) + B_y \cos(2\pi\bar{x}_4) + l_y \\
z(\bar{x}_4) &= z_0 + A_z \sin(2\pi\bar{x}_4) + B_z \cos(2\pi\bar{x}_4) + l_z,
\end{aligned} \quad (1)
$$

where $\bar{x}_4 = \mathbf{q} \cdot \mathbf{r}_0 = q_z \cdot (z_0 + l_z)$, and l_x, l_y and l_z are integer numbers. The atomic positions of the basic crystal structure (without modulation), *i.e.* x_0, y_0, z_0 and the modulation amplitudes A_i, B_i are given in fractional coordinates. The values of the atomic positions and the modulation amplitudes determined from refinement for all the ions in CaMn$_7$O$_{12}$ at T = 10 K are given in Table 2.

For CaMn$_7$O$_{12}$ the average FWHM of the satellite peaks (0.013°) is considerably larger then the average FWHM of fundamental reflections (0.008°). It is also important to note that the satellite peaks observed in CaCu$_x$Mn$_{7-x}$O$_{12}$ ($x = 0.1$) are broader than those observed in CaMn$_7$O$_{12}$. Different FWHM values were assumed for fundamental and satellite reflections during refinement with the program *JANA*2006.

The fits performed for CaMn$_7$O$_{12}$ at higher temperatures ($10 < T < 210$ K) give amplitude values with similar mutual proportions. The modulation amplitudes decrease with increasing temperature and they vanish above 250 K. Fits assuming the same type of atomic position modulations were also performed for CaCu$_x$Mn$_{7-x}$O$_{12}$ ($x = 0.1$). The values of q_p (see Fig. 3) give a good description of the satellite peak

positions. The modulation amplitudes determined for CaCu$_x$Mn$_{7-x}$O$_{12}$ ($x = 0.1$) show large variations for synchrotron radiation diffraction patterns obtained at closely spaced temperature values. The modulation amplitudes show large statistical errors owing to the weaker statistical accuracy of the synchrotron radiation diffraction data for CaCu$_x$Mn$_{7-x}$O$_{12}$ ($x = 0.1$). The refinement results for CaCu$_x$Mn$_{7-x}$O$_{12}$ ($x = 0.1$) are not shown in Table 2.

The Mn1 positions (perovskite *A* sublattice) are surrounded by 12 oxygen ions which form a tetracapped rhombic prism in the basic structure (Bochu *et al.*, 1980). There are two nearest-neighbour Mn1—O1 and two Mn1—O2 distances with relatively weak modulation, as shown in Fig. 4(*a*). The Mn2 positions (perovskite *B* sublattice) are surrounded by six oxygen ions which form a Jahn–Teller distorted (apically

Figure 4
Nearest-neighbour Mn—O bond-length modulations in CaMn$_7$O$_{12}$ are shown for Mn1, Mn2 and Mn3 positions in panels *a*, *b* and *c*. The horizontal axis shows the scale in relative units $t = \bar{x}_4$ [see equation (1)]. Results obtained from the analysis of synchrotron radiation diffraction data at T = 10 K (see text). This figure is in colour in the electronic version of this paper.

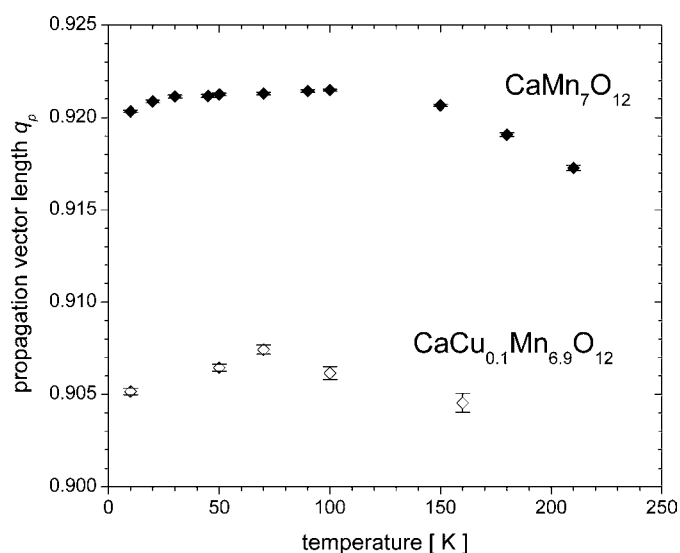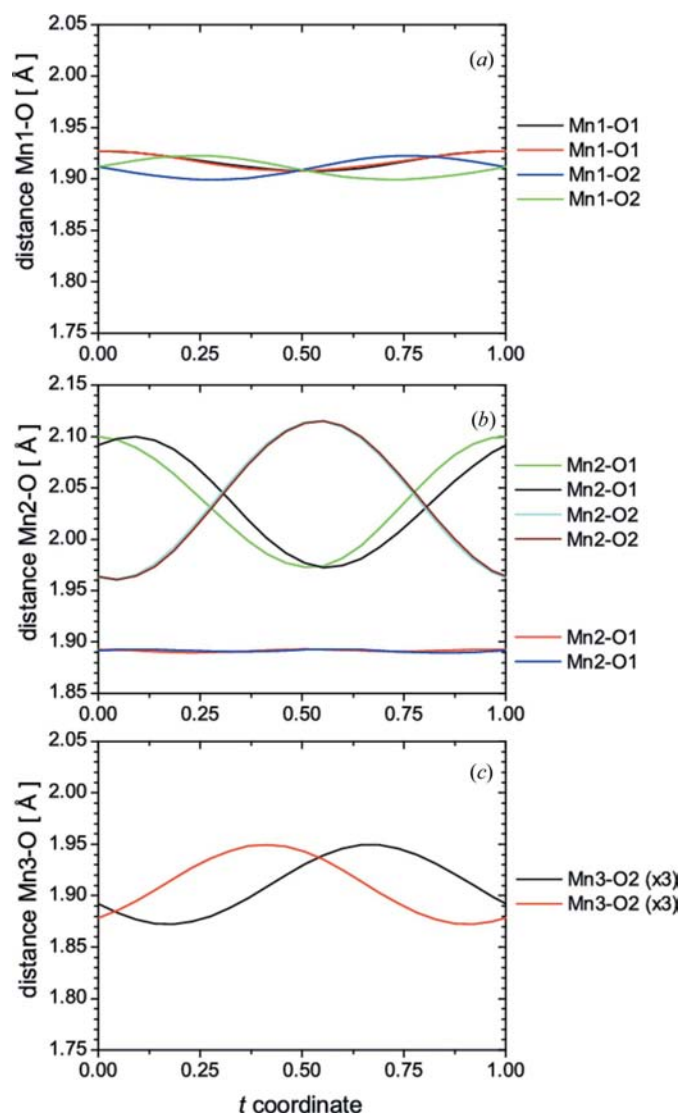**Figure 3**
Temperature dependence of the propagation vector length q_p describing the atomic position modulations in CaCu$_x$Mn$_{7-x}$O$_{12}$ ($x = 0$ and 0.1). Results obtained from the analysis of synchrotron radiation powder diffraction data (see text).

contracted) octahedron in the basic structure. Fig. 4(b) shows important differences in the Mn—O bond-length modulation, i.e. a large amplitude of the modulation of the four longer equatorial Mn2—O1 and Mn2—O2 bonds (apically distorted $Mn^{3+}O_6$ octahedra) and much weaker modulation of the two short apical Mn2—O1 bonds. The Mn3 positions (perovskite B sublattice) are surrounded by six oxygen ions with equal Mn3—O2 bond length in the basic structure. The Mn3—O2 bonds show a relatively large modulation amplitude, as given in Fig. 4(c).

Selected Mn—O distances of the basic crystal structure of $CaMn_7O_{12}$ obtained at 10 K are gathered in Table 3.

The modulation of the Mn—O—Mn angles between Mn1, Mn2 and Mn3, and O1, O2 positions in $CaMn_7O_{12}$ at 10 K are shown as a function of the t coordinate in Figs. 5(a)–(c). One
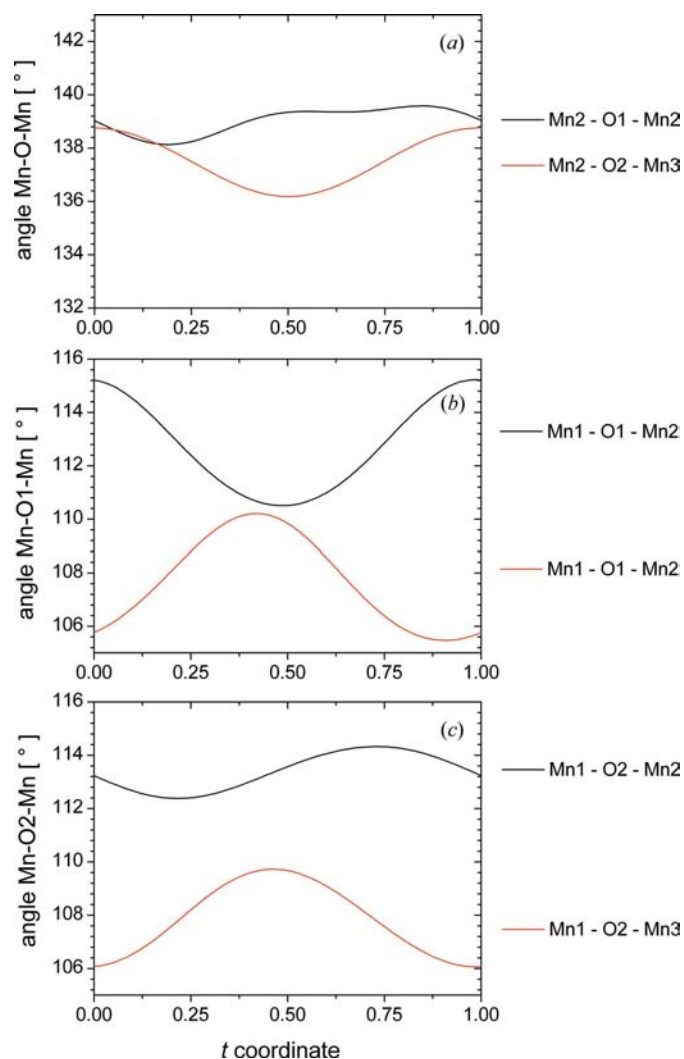
Table 3
Selected neighbor Mn—O distances in the basic crystal $CaMn_7O_{12}$ structure determined at 10 K.

Bond	Length (Å)	
Mn1—O1	1.908 (3)	×2
Mn1—O2	1.902 (2)	×2
Mn1—O1	2.715 (3)	×2
Mn1—O2	2.803 (2)	×2
Mn1—O1	3.288 (2)	×2
Mn1—O2	3.327 (3)	×2
Mn2—O1	2.042 (3)	×2
Mn2—O2	2.044 (3)	×2
Mn2—O1	1.890 (3)	×2
Mn3—O2	1.912 (3)	×6

can see important changes of the Mn—O—Mn angles that may influence the magnetic interactions in $CaMn_7O_{12}$.

The $Mn2O_6$ and $Mn3O_6$ octahedra also show the modulation of the O—Mn—O bond angles close to 90° (inside the octahedra, see Fig. 6).

The O—Mn—O angles close to 180° also show important modulation, as shown in Fig. 7.

The bond-valence sum was calculated for the Mn ions in $CaMn_7O_{12}$ by using the program JANA2006. The bond-valence parameters were taken from Brown & Altermatt (1985). These calculations gave average bond-valence sums of 2.916, 3.297 and 3.896 for Mn1, Mn2 and Mn3. The bond-
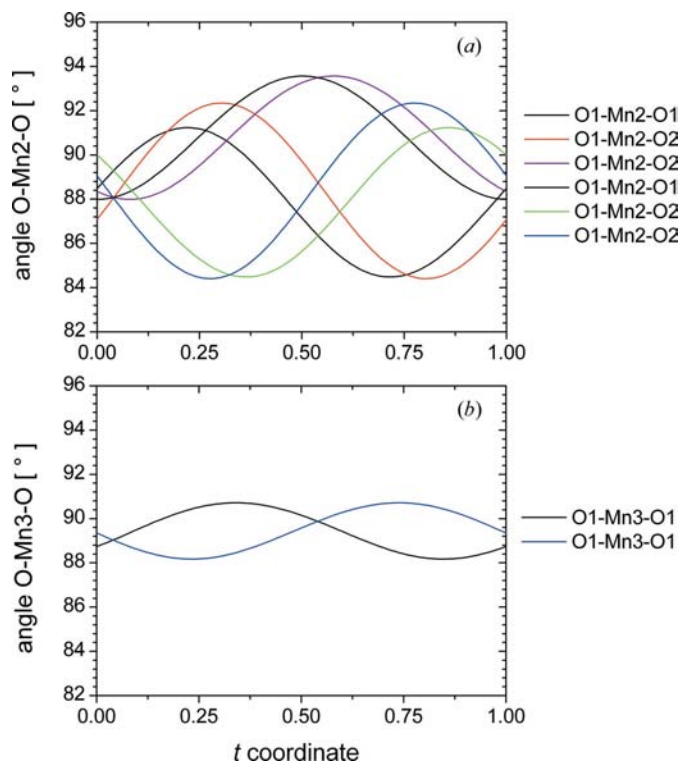

Figure 5
Modulation of the nearest-neighbour Mn—O—Mn bond angles in $CaMn_7O_{12}$ are shown for Mn1, Mn2 and Mn3 positions in panels a, b and c. The horizontal axis shows the scale in relative units $t = \bar{x}_4$ [see equation (1)]. Results obtained from the analysis of synchrotron radiation diffraction data at $T = 10$ K (see text). This figure is in colour in the electronic version of this paper.

Figure 6
Modulation of the nearest-neighbour O—Mn—O bond angles close to 90° (inside MnO_6 octahedra) in $CaMn_7O_{12}$ are shown for Mn2 and Mn3 positions in panels a and b, respectively. The horizontal axis shows the scale in relative units $t = \bar{x}_4$ [see equation (1)]. Results obtained from the analysis of synchrotron radiation diffraction data at $T = 10$ K (see text). This figure is in colour in the electronic version of this paper.

valence sum amplitudes are 0.039, 0.040 and 0.234 for Mn1, Mn2 and Mn3. The observed modulation of the Mn—O bond lengths and Mn—O—Mn angles may influence the ionic charges and also the magnetic interactions in the $CaCu_xMn_{7-x}O_{12}$ series. This finding prompted us to revisit the detailed analysis of the $CaCu_xMn_{7-x}O_{12}$ system.

3.2. Magnetic moments modulation

Below T_N = 89 K long-range magnetic ordering is observed in $CaMn_7O_{12}$ (Przenioso et al., 1999, 2000). The present neutron diffraction measurements show the onset of the long-range magnetic ordering at T_N equal to 90.4, 89.2 and 78.1 K for $CaCu_xMn_{7-x}O_{12}$, x = 0, 0.1 and 0.23. In $CaCu_xMn_{7-x}O_{12}$

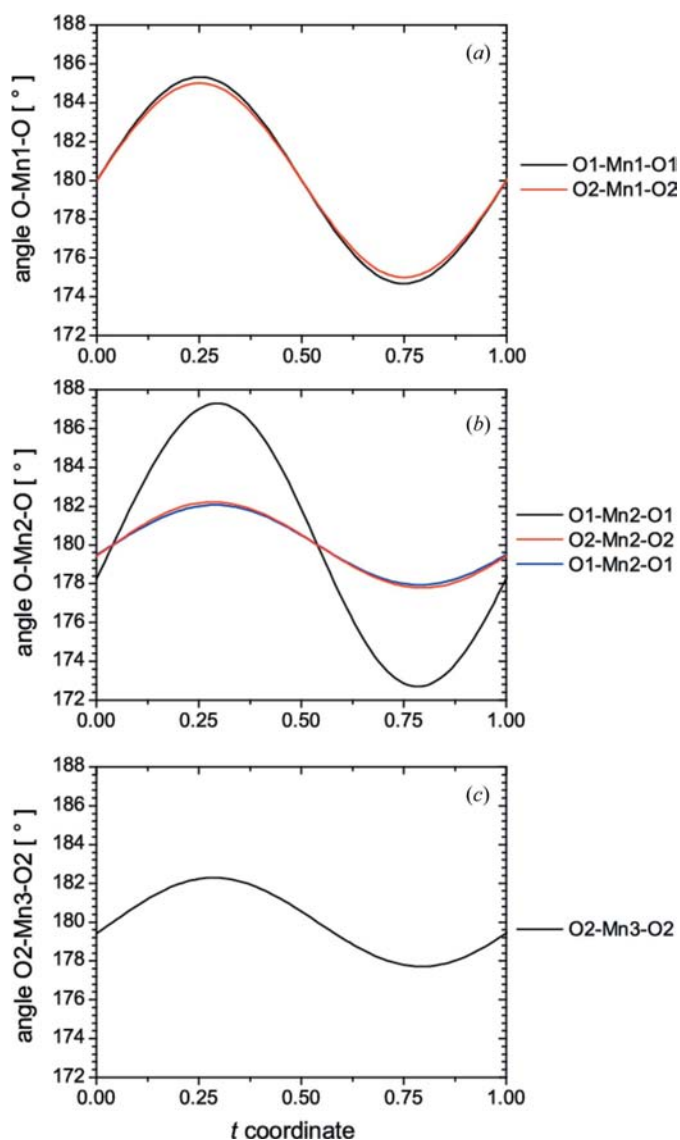**Figure 7**
Modulation of the nearest-neighbour O—Mn—O bond angles close to 180° (inside MnO$_6$ octahedra) in $CaMn_7O_{12}$ are shown for Mn1, Mn2 and Mn3 positions in panels a, b and c. The horizontal axis shows the scale in relative units $t = \bar{x}_4$ [see equation (1)]. Results obtained from the analysis of synchrotron radiation diffraction data at T = 10 K (see text). This figure is in colour in the electronic version of this paper.

Table 4
Values of the propagation vector length describing the modulation of magnetic moments, q_m and atomic positions, q_p, in $CaCu_xMn_{7-x}O_{12}$ compounds.

Values of q_m are determined from neutron diffraction measurements at temperature T_1, while q_p are determined from synchrotron radiation diffraction measurements at temperature T_2. The lattice parameter c obtained at temperature T_2 is also given.

x	T_1 (K)	q_m	$2(1 - q_m)$	T_2 (K)	q_p	$(1 - q_p)$	c (Å)
0.0	60.0	0.9604 (4)	0.0792 (8)	70.0	0.9213 (1)	0.0787 (1)	6.343566 (1)
0.1	58.0	0.9537 (4)	0.0926 (8)	70.0	0.9081 (2)	0.0919 (2)	6.342108 (2)
0.23	53.5	0.9466 (4)	0.1068 (8)	70.0	–	–	–

(x = 0, 0.1 and 0.23) compounds two magnetic phases are observed: a ferrimagnetic phase (α phase) and an incommensurate modulated phase (β phase), i.e. magnetic ordering is similar to that observed in $CaMn_7O_{12}$ (Przenioso et al., 1999). It was not possible to properly index the magnetic satellites of the β phase in $CaMn_7O_{12}$, see Fig. 2 in Przenioso et al. (1999).

The present neutron diffraction patterns obtained for $CaCu_xMn_{7-x}O_{12}$ (x = 0, 0.1 and 0.23) at temperatures between 50 K and T_N have been analysed by using the programs FullProf (Rodríguez-Carvajal, 1993) and JANA2006 (Petricek et al., 2006). For each temperature the values of the lattice parameters a and c were determined by refining against the synchrotron radiation diffraction patterns using the Rietveld package FullProf (Rodríguez-Carvajal, 1993). The nuclear and magnetic Bragg peaks were indexed with the pattern-matching mode of the program JANA2006, using fixed values of the lattice parameters as obtained from the FullProf refinements. The observed Bragg peaks were indexed as $(h, k, l \pm q_m)$. The agreement of the calculated and observed peak positions for $CaCu_xMn_{7-x}O_{12}$ (x = 0, 0.1 and 0.23) is shown in Fig. 8. The values of q_m for $CaCu_xMn_{7-x}O_{12}$, with x = 0, 0.1 and 0.23, are given in Table 4. This indexing solution with fixed q_m agrees within experimental error with the neutron diffraction data observed at all temperatures: 50 K < T < T_N.

At this stage the propagation vector of the modulated magnetic structure is determined, however, this is not a full solution of the magnetic ordering.

The magnetic satellite peak $(0, 0, 1 + q_m) \simeq (0, 0, 1.96)$ shown in Fig. 8 should be associated with another magnetic satellite peak at $(0, 0, 1 - q_m) \simeq (0, 0, 0.04)$, which is outside the present neutron diffraction data range. Such low s values also exceed the lower limits of our previous SANS measurements performed with $CaMn_7O_{12}$ (Przenioso et al., 2000). The present indexing solution with a single q_m value cannot explain the low-angle magnetic satellite observed near $(0, 0, 0.12)$ for 50 K < T < T_N in $CaMn_7O_{12}$ (Przenioso et al., 1999, 2000). This magnetic peak could be indexed as the third-order satellite, i.e. $(0, 0, 3(1 - q_m))$. In such a case one should also expect third-order satellites at higher scattering angles, however, such third-order satellites are not detected in the present neutron powder patterns shown in Fig. 8. They might have small intensities lying below the detection threshold of the present neutron powder diffraction experiment. Thus, the

existence of such third-order satellites in neutron diffraction patterns remains an open question.

4. Discussion

The present studies confirm the relation between modulated magnetic ordering and magnetoelectric coupling which is predicted by theoretical arguments (Katsura *et al.*, 2005; Mostovoy, 2006). The magnetic modulation was observed experimentally in several multiferroic oxide materials, *e.g.* BiFeO$_3$ (Sosnowska *et al.*, 1982; Teague *et al.*, 1970), TbMnO$_3$ (Kimura *et al.*, 2003), Ba$_2$Mg$_2$Fe$_{12}$O$_{22}$ (Ishiwata *et al.*, 2008) and CuO (Kimura *et al.*, 2008).

The present study of CaCu$_x$Mn$_{7-x}$O$_{12}$ has shown a relation between the modulation of the atomic positions described by q_p and the magnetic modulation described by q_m. The values given in Table 4 fulfill the relation $(1 - q_p) = 2(1 - q_m)$ within experimental error for CaCu$_x$Mn$_{7-x}$O$_{12}$, $x = 0$ and 0.1. The modulation length of the magnetic ordering is therefore two times longer than the modulation length of the atomic displacements.

A theoretical description shows that a magnetic modulation with wavevector q can be associated with a modulation of atomic positions with wavevector $2q$ (Lovesey & Collins, 1996) for a system with:
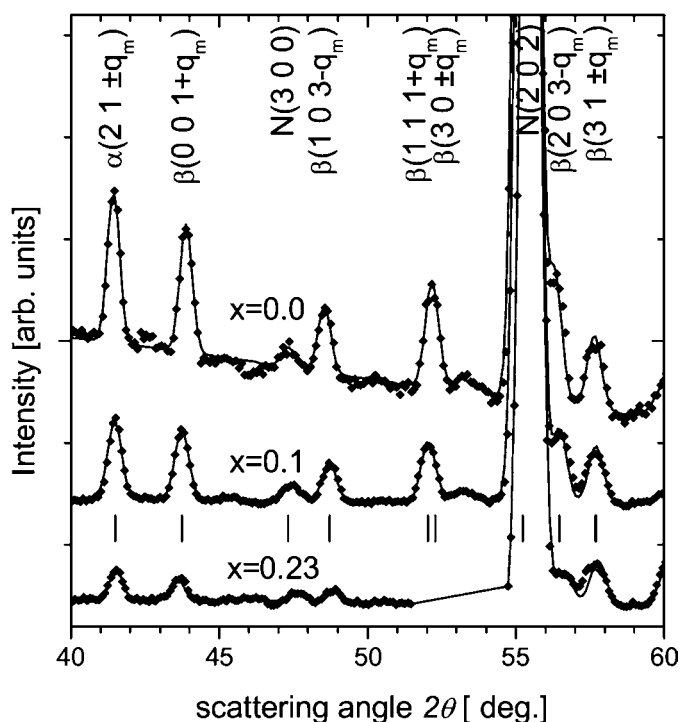

Figure 8
Selected parts of the neutron powder diffraction patterns of CaCu$_x$Mn$_{7-x}$O$_{12}$ with $x = 0$, 0.1 and 0.23 observed at $T = 60$ K. The indices of the Bragg peaks are given above the plots and the calculated peak positions are indicated as tick marks below the central plot. The symbols N, α and β relate to the nuclear, magnetic α phase and magnetic β phase. Part of the CaCu$_x$Mn$_{7-x}$O$_{12}$ ($x = 0.23$) pattern between 51.5 and 55° has been removed because of technical problems with the detectors.

(i) transverse modulation of the ordered magnetic moments $\mu_z = \mu_0 \sin(q_m x)$;
(ii) Heisenberg exchange interaction $H = -J(d)\mu_n\mu_{n+1}$;
(iii) linear dependence of the exchange integral $J(d)$ on the interatomic distance d.

The magnetic modulation observed with the wavevector q_m couples to a longitudinal modulation of the atomic positions described by a wavevector $q_p = 2q_m$. This has been observed in metals, *i.e.* chromium (Tsunoda *et al.*, 1974; Fawcett, 1988) and thulium (Bohr *et al.*, 1990) and also in Kondo systems Ce(Ru$_{1-x}$Rh$_x$)Si$_2$ (Tabata *et al.*, 2005) and multiferroic oxides CuFe$_{1-x}$Al$_x$O$_2$ (Nakajima *et al.*, 2008). In all these materials the modulation of the magnetic moments and the modulation of the atomic positions appear below the same temperature T_N.

In the present case of CaCu$_x$Mn$_{7-x}$O$_{12}$ ($x = 0$ and 0.1) the magnetic moment and atomic position modulations are observed at markedly different transition temperatures, *i.e.* ~ 250 and ~ 90 K. It is proposed that the atomic position modulation is the driving force which determines the wavevector of the magnetic ordering for CaCu$_x$Mn$_{7-x}$O$_{12}$ ($x = 0$ and 0.1). It is not clear if this conclusion is also valid for CaCu$_x$Mn$_{7-x}$O$_{12}$ ($x = 0.23$), because the satellites due to atomic position modulation have not been detected in the synchrotron radiation diffraction patterns. However, the magnetic ordering in CaCu$_x$Mn$_{7-x}$O$_{12}$ ($x = 0.23$) is clearly observed and it is identified that the observed values of q_m show linear behaviour with respect to the Cu content x (see Table 4).

The present study does not give a full description of the modulated magnetic ordering of CaCu$_x$Mn$_{7-x}$O$_{12}$ compounds. The propagation vector q_m has been determined and it has been concluded that the magnetic ordering may be of spin-density wave type in analogy with chromium. This study shows many similarities between the magnetic ordering of undoped and Cu doped CaMn$_7$O$_{12}$ compounds. These similarities suggest that the electronic and magnetic properties of the CaCu$_x$Mn$_{7-x}$O$_{12}$ compounds may be also similar to those of undoped CaMn$_7$O$_{12}$. Since pure CaMn$_7$O$_{12}$ reveals simultaneous colossal dielectric behaviour and modulated magnetic ordering would be interesting to study the relationship between the dielectric and magnetic properties of the CaCu$_x$Mn$_{7-x}$O$_{12}$ series. It is conceivable that magnetoelectric coupling also exists in CaCu$_x$Mn$_{7-x}$O$_{12}$.

References

Bochu, B., Buevoz, J., Chenavas, J., Collomb, A., Joubert, J. & Marezio, M. (1980). *Solid State Commun.* **36**, 133–138.

Bohr, J., Gibbs, D. & Huang, K. (1990). *Phys. Rev. B*, **42**, 4322–4328.

Brown, I. D. & Altermatt, D. (1985). *Acta Cryst.* B**41**, 244–247.

Castro-Couceiro, A., Yáñez-Vilar, S., Rivas-Murias, B., Fondado, A., Mira, J., Rivas, J. & Señarís-Rodríguez, M. A. (2006). *J. Phys. Condens. Matter*, **18**, 3803–3815.

Fawcett, E. (1988). *Rev. Mod. Phys.* **60**, 209–283.

Fitch, A. N. (2004). *J. Res. Natl. Inst. Stand. Technol.* **109**, 133–142.

Ishiwata, S., Taguchi, Y., Murakawa, H., Onose, Y. & Tokura, Y. (2008). *Science*, **319**, 1643–1646.

Katsura, H., Nagaosa, N. & Balatsky, A. V. (2005). *Phys. Rev. Lett.* **95**, 1–4.

Kimura, T., Goto, T., Shintani, H., Ishizaka, K., Arima, T. & Tokura, Y. (2003). *Nature*, **426**, 55–58.

Kimura, T., Sekio, Y., Nakamura, H., Siegrist, T. & Ramirez, A. P. (2008). *Nature Mater.* **7**, 291–294.

Lovesey, S. W. & Collins, S. P. (1996). *X-ray Scattering and Absorption by Magnetic Materials.* Oxford University Press.

Mostovoy, M. (2006). *Phys. Rev. Lett.* **96**, 067601.

Nakajima, T., Mitsuda, S., Inami, T., Terada, N., Ohsumi, H., Prokes, K. & Podlesnyak, A. (2008). *Phys. Rev. B*, **78**, 024106.

Petricek, V., Dusek, M. & Palatinus, L. (2006). *JANA*2006. Institute of Physics, Prague, Czech Republic.

Presniakov, I. A., Rusakov, V. S., Gubaidulina, T. V., Sobolev, A. V., Baranov, A. V., Demazeau, G., Volkova, O. S., Cherepanov, V. M., Goodilin, E. A., Knot'ko, A. V. & Isobe, M. (2007). *Phys. Rev. B*, **76**, 214407.

Prodi, A., Allodi, G., Gilioli, E., Licci, F., Marezio, M., Bolzoni, F., Gauzzi, A. & De Renzi, R. (2006). *Phys. Rev. B Condens. Matter*, **374–375**, 55–58.

Przeniosło, R., Sosnowska, I., Hohlwein, D., Hauß, T. & Troyanchuk, I. O. (1999). *Solid State Commun.* **111**, 687–692.

Przeniosło, R., Sosnowska, I., Strunz, P., Hohlwein, D., Hauß, T. & Troyanchuk, I. O. (2000). *Physica B*, **276**, 547–548.

Rietveld, H. M. (1969). *J. Appl. Cryst.* **2**, 65–71.

Rodríguez-Carvajal, J. (1993). *Phys. B*, **192**, 55–69.

Sánchez-Andújar, M., Yáñez-Vilar, S., Biskup, N., Castro-García, S., Mira, J., Rivas, J. & Señarís-Rodríguez, M. A. (2009). *J. Magn. Magn. Mater.* **321**, 1739–1742.

Sławiński, W., Przeniosło, R., Sosnowska, I., Bieringer, M., Margiolaki, I., Fitch, A. N. & Suard, E. (2006). *J. Solid State Chem.* **179**, 2443–2451.

Sławiński, W., Przeniosło, R., Sosnowska, I., Bieringer, M., Margiolaki, I., Fitch, A. N. & Suard, E. (2008). *J. Phys. Condens. Matter*, **20**, 104239.

Smaalen, S. van (2007). *Incommensurate Crystallography*, pp. 2–4. Oxford University Press.

Sosnowska, I., Neumaier, T. P. & Steichele, E. (1982). *J. Phys. C Solid State Phys.* **15**, 4835–4846.

Tabata, Y., Taniguchi, T., Kawarazaki, S., Narumi, Y., Kimura, S., Tanaka, Y., Katsumata, K., Ishikawa, T., Staub, U., Kohgi, M. & Iwasa, K. (2005). *Phys. B Condens. Matter*, **359–361**, 260–262.

Teague, J., Gerson, R. & James, W. (1970). *Solid State Commun.* **8**, 1073–1074.

Tsunoda, Y., Mori, M., Kunitomi, N., Teraoka, Y. & Kanamori, J. (1974). *Solid State Commun.* **14**, 287–289.

Vasiliev, A. N. & Volkova, O. S. (2007). *Low Temp. Phys.* **33**, 895–914.

Volkova, O., Arango, Y., Tristan, N., Kataev, V., Gudilin, E., Meier, D., Lorenz, T., Buchner, B. & Vasil'ev, A. (2005). *JETP Lett.* **82**, 444–446.

Volkova, O., Klimov, K., Savelieva, O., Tristan, N., Goodilin, E., Buechner, B. & Vasiliev, A. (2006). *J. Magn. Magn. Mater.* **300**, e134–136.

Yáñez-Vilar, S., Castro-Couceiro, A., Rivas-Murias, B., Fondado, A., Mira, J., Rivas, J. & Señarís-Rodríguez, M. A. (2005). *Z. Anorg. Allg. Chem.* **631**, 2192–2196.

Zeng, Z., Greenblatt, M., Sunstrom, J. E., Croft, M. & Khalid, S. (1999). *J. Solid State Chem.* **147**, 185–198.